Ab Initio Simulation of Si-Doped Hydroxyapatite

R. Astala, L. Calderín, X. Yin, and M. J. Stott*

Department of Physics, Queen's University, Kingston, Ontario K7L 3N6, Canada

Received September 2, 2005. Revised Manuscript Received October 12, 2005

Si-doped hydroxyapatite is a bioceramic useful as a bone repair material retaining the hexagonal structure of hydroxyapatite up to about 2 wt % Si. Different mechanisms for charge compensation for the SiO_4^{4-} ion substituting for the PO_4^{3-} have been proposed. Also, variations are reported in the dependence of the lattice parameters on the Si doping. These may be a result of different charge compensation mechanisms which may in turn depend on the method of preparation of the material. Calculation using ab initio total energy methods have been performed to investigate different mechanisms for charge compensation in Si-doped hydroxyapatite. Mechanisms involving an OH vacancy, an oxygen vacancy, and an additional hydrogen are studied. These mechanisms correspond to different degrees of dehydration and, consequently, depend on water partial pressure and chemical potential. Full relaxation of the atomic positions and the unit cell parameters was performed, and ground-state energies of the equilibrium structures, equilibrium lattice parameters, and atomic arrangements were obtained. The results indicate that which charge compensation mechanism is stable depends on the chemical potential of water. For small values of the water chemical potential the mechanism involving an OH vacancy is stable, but for larger values the mechanism leading to the formation of $HSiO_4$ is stable. The other mechanisms considered are unstable.

I. Introduction

Hydroxyapatite (HA), $Ca_5(PO_4)_3OH$, is the main inorganic component of animal bone and teeth and also occurs naturally as a rare mineral. The crystal structure of HA is hexagonal with two formula units per unit cell, although monoclinic structures with four formula units per unit cell have also been reported in which the *b* lattice parameter is doubled.[1−5] The observation of different crystal structures may be due to imperfect stoichiometry, as it is well-known that HA is often deficient in OH^-, HPO_4^{2-} ions can be present, and other anions such as F^- can substitute for OH^-. In bone mineral there are a variety of dopants, the main one being CO_3^{2-} of which there is approximately 7 wt %.[6] Other trace elements such as Si are at lower concentrations, but even so, these low levels of Si have important effects on skeletal development.[7]

There are also a number of Si-doped calcium phosphates that are promising bioceramic materials for use in bone repair. Multiphase Si-stabilized calcium phosphate bulk ceramics have been prepared by sintering at about 1000 °C a finely dispersed colloidal solution of HA and silica. Similar material is prepared in thin film form on a quartz substrate. The main features of these materials are a composition with approximately 75% silicon-stabilized α-tricalcium phosphate (Si-TCP) with the remainder being mainly Si-substituted HA (Si−HA) and an interconnected surface morphology. The presence of Si−TCP with the α-phase crystal structure is unexpected because α-TCP is the high-temperature tricalcium phosphate phase and it is β-TCP that is stable at room temperature. These materials exhibit unique biological activity taking part fully in the body's bone remodeling process, and it is believed to be the Si−TCP component that is responsible for this bioactivity.[8] The bioactive glasses based on silicates such as Bioglass are another important group of synthetic bone repair materials.[9] These are used in coatings which stimulate the formation of a bond between tissue and metal implants.

A Si−HA was prepared and studied by Ruys,[10] but the Si−HA was just one of several phases in a multiphase mixture. Subsequently, Gibson et al.[11] prepared Si−HA which for small Si concentrations of 0.4 wt % was a single phase with the same hexagonal crystal structure as HA. This material is promoted as a biologically effective source of in vivo silicon without compromising the chemical and physical properties of HA as present in bone. Whereas the Si−HA material at least for low doping is single phase, the Si-stabilized calcium phosphate containing Si−TCP described earlier is multiphase, one component of which is HA-like but containing some Si. The Si content of this HA phase or its overall stoichiometry is not known at this time as it is just one of several phases.

* To whom correspondence should be addressed. E-mail: stott@mjs.phy.queensu.ca.

(1) Elliott, J. C. *Structure and Chemistry of the Apatites and Other Calcium Orthophosphates*; Elsevier: Amsterdam, 1994.
(2) Morgan, H.; Wilson, R. M.; Elliott, J. C.; Dowker, S. E. P.; Anderson, P. *Biomaterials* **2000**, *21*, 617.
(3) Ikoma, T.; Yamazaki, A.; Nakamura, S.; Akao, M. *J. Solid State Chem.* **1999**, *144*, 272.
(4) Elliott, J. C.; Mackie, P. E.; Young, R. A. *Science* **1973**, *180*, 1055.
(5) Haverty, D.; Tofail, S. A. M.; Stanton, K. T.; McMonagle, J. B. *Phys. Rev. B* **2005**, *71*, 094103.
(6) Dorozhkin, S. V.; Epple, M. *Angew. Chem., Int. Ed.* **2002**, *41*, 3131.
(7) Carlisle, E. M. *Science* **1972**, *62*, 178−619.
(8) Langstaff, S.; Sayer, M.; Smith, T. J. N.; Pugh, S. M. *Biomaterials* **2001**, *22*, 135.
(9) Hench, L. L. *J. Am. Ceram. Soc.* **1991**, *74*, 1487−510.
(10) Ruys, A. J. *J. Aust. Ceram. Soc.* **1993**, *29*, 71−80.
(11) Gibson, I. R.; Best, S. M.; Bonfield, W. *J. Biomed. Mater. Res.* **1999**, *44*, 422−428.

10.1021/cm051989x CCC: $33.50
Published on Web 12/18/2005

The Si−HA material of interest was first reported by Gibson et al.[11] and prepared using an aqueous precipitation method with the amounts of ingredients $Ca(OH)_2$, H_3PO_4, and Si−acetate chosen so that the ratio $Ca/(Si + P) = 1.67$ as in pure HA. The resulting precipitate was sintered at 1200 °C in air. Chemical analysis gave a Si content close to the target value of 0.4 wt %, which amounts on average to about one Si substitution per 14 $Ca_5(PO_4)_3OH$ formula units or per seven HA unit cells. X-ray diffraction showed that no phases were present other than a hexagonal HA-like phase. Small changes in lattice parameters from HA were found with *a* decreasing and *c* increasing with a very small reduction in volume. Rietveld refinement of the X-ray diffraction data also gave a reduction of the occupancy of the OH sites on incorporation of Si into the HA structure which, it was noted, is consistent with Si substituting for P in a PO_4 group with an associated OH vacancy in the anion column along the *c* axis providing local charge compensation. Kim et al.[12] investigated Si−HA also prepared using an aqueous precipitation method but with much higher Si concentrations, close to the targeted 2 and 4 wt %. They sintered at different temperatures in the range 1000−1500 °C. The 2 wt % material retained single phase HA-like structure for sintering temperatures up to 1200 °C, beyond which other phases appeared, and the 4 wt % Si sample decomposed before being fully sintered. Thus, the limit for the incorporation of Si into the HA lattice without the formation of other phases seems to be roughly 2 wt %. Refinement of X-ray diffraction data for the 2 wt % material gave an increase in the *c* lattice parameter as for the more dilute Si−HA described above but, in contrast, a small increase in *a*. However, the concentration of 2 wt % Si corresponds on average to a Si substitution per two hexagonal HA cells. Leventouri et al.[13] prepared Si−HA with a target of 0.4 wt % Si using a method similar to Gibson et al.[11] and obtained results for lattice parameter changes similar to those of these authors, except for a much smaller decrease in the *a* parameter. They also found a reduction in the OH occupancy upon doping, suggesting charge compensation involving an OH vacancy, but their undoped sample had an OH occupancy of only 0.30, much lower than the ideal value of 0.50. Ruys[10] assumed charge compensation by OH vacancies, but the $Ca/(Si + P)$ ratio was not maintained at 1.67 and their material contained other phases in addition to Si−HA. However, other charge compensation mechanisms are possible. Most recently, Arcos et al.[14] prepared Si−HA with 0.97 wt % Si with a high-temperature solid-state reaction. The material was prefired at 900 °C and then fired at 1200 °C for a longer period, and the process was repeated until a single HA-like phase was obtained. The lattice parameter changes were different again with very small decreases in *c* as well as *a*. Fourier transform infrared spectroscopy showed the presence of HPO_4, and analysis of X-ray and neutron scattering data indicated an increase in the OH/O ratio on Si doping. This is contrary to expectations if the charge compensation mechanism for the Si substitution involves an OH vacancy, and these authors suggested that H rather than an OH vacancy may be involved in charge compensation.

It is generally expected that Si doping of calcium phosphates in these bioceramics would lead to Si substituting for P and a SiO_4^{4-} ion replacing a PO_4^{3-} ion. Consequently, an extra electron is required for the SiO_4^{4-} ion over the PO_4^{3-} if there is not to be a substantial cost in energy. This charge compensation involves other charged defects and can take place in a number of ways. Charge compensation of Si dopants in α-TCP has been studied by two of the authors[15] using ab initio total energy methods based on density functional theory (DFT) to simulate the electronic structure and atomic arrangement. The two mechanisms for charge compensation that were investigated involved either an excess calcium atom or an oxygen vacancy per two neighboring SiO_4 substitutions. The first principles or ab initio methods based on a quantum mechanical treatment of the electrons yield reliable total energies and the forces on the atoms, which can be used to obtain the equilibrium arrangement of atoms. However, the energies of the two charge compensation mechanisms cannot easily be compared directly because different sets of atoms are involved. A comparison can be made if the chemical potentials of the individual atoms are known, but this is usually not the case. Nevertheless, an approximate comparison is possible if the energy is known for an intermediate stable compound which links the two systems. For Si−TCP this compound was assumed to be solid CaO. This observation allowed Yin and Stott[15] to conclude that the charge compensation by excess calcium is energetically favored over the oxygen vacancy mechanism by about 1.6 eV per two SiO_4. The present paper reports a similar ab initio investigation of Si−HA in which different possible charge compensation mechanisms can be compared. Three different scenarios are considered: compensation of SiO_4 impurities by excess H in HPO_4^{2-} or $HSiO_4^{3-}$ groups, by OH vacancies, or by O vacancies. These mechanisms again involve different sets of atoms, and a comparison of the energies cannot be made directly. But, a simplifying feature of these systems is that they are related to one another by different amounts of dissociated water in the lattice. The chemical potential of water [$\mu(H_2O)$] is a function of the water vapor partial pressure. Although the $\mu(H_2O)$ under the circumstances of the preparation of the materials is not readily available, firm conclusions can be drawn on the relative stability of the systems as a function of $\mu(H_2O)$. The investigation should be useful in the interpretation of the experimental data on Si−HA, where there are discrepancies, as presented above, to be resolved.

In summary, this paper presents results of an ab initio investigation of various possible scenarios for the Si doping of HA. These involve different charge defects for the charge compensation of Si substituting for P. For each charge compensation mechanism there are several possible atomic arrangements. For each of these arrangements the calculations give total energies which can be ranked to identify the most

(12) Kim, S. R.; H., L. J.; Kim, Y. T.; Riu, D. H.; Jung, S. J.; Lee, Y. J.; Chung, S. C.; Kim, Y. H. *Biomaterials* **2003**, *24*, 1389−1398.
(13) Leventouri, T.; Bunaciu, C. E.; Perdikatsis, V. *Biomaterials* **2003**, *24*, 4205−4211.
(14) Arcos, D.; Rodríguez-Carvajal, J.; Vallet-Regí *Solid State Sci.* **2004**, *6*, 987−994.
(15) Yin, X.; Stott *J. Chem. Phys.* **2005**, *122*, 024709−9.

stable ones. The calculations also give changes of lattice parameters with doping, and the magnitude and sign of the changes depend on the type of charge compensation mechanism and on the particular atomic arrangement for each type. The results suggest that the charge compensation mechanism which prevails, and consequently the lattice parameter changes, will depend on the availability of water. This in turn may provide explanations for the range of results reported by groups for Si−HA materials prepared in different ways.

The theoretical methods are described in the next section. The presentation of the results of the simulations for the different charge compensation mechanisms follows. A comparison of the theoretical results among themselves and with the experimental data is made in the discussion, and conclusions are drawn in the final section.

II. Methods

A. Computational Techniques. DFT[16,17] as implemented in the SIESTA code[18] was used for all the calculations. This approach solves the one-particle problem self-consistently using a linear combination of pseudoatom orbitals. Geometry optimization of both atomic positions and lattice constants was performed for the structures considered. The conjugate gradients method was used.[19] The optimization was based on total energy calculations performed using the generalized gradient approximation (GGA) for exchange and correlation with the Perdew−Burke−Ernzerhof functional.[20] Some calculations were also performed with the local density approximation (LDA) for exchange and correlation, and the same trends in total energy and lattice parameter changes were found as for the GGA. However, the LDA generally tends to overbind and, for example, severely overestimates binding energies for H_2O molecules. Consequently, it is likely to be unreliable for the energetics of reactions involving H_2O that are important in this study, and apart from a few instances only the GGA results are reported.

Norm-conserving Troullier−Martins pseudopotentials[21] were adopted in the present work. The same pseudopotentials and, except for H, the same basis sets are used as in our earlier work on α- and β-tricalcium phosphate and on apatites, and full details are given there.[22,23] It was found necessary to include explicitly in the calculations the semicore 3s and 3p electrons of Ca. The pseudopotentials were generated using the following reference configurations: $3s^2 3p^6$ for Ca^{2+}, $3s^1 3p^{1.75} 3d^{0.25}$ for P^{2+}, $2s^2 2p^4$ for O, and $3s^1 3p^{0.75} 3d^{0.25}$ for Si^{2+}. The core radii used were 1.80 au for the s, p, d, and f states of Ca; 1.60 au for the s, p, d, and f states of P; 1.15 au for the s, p, d, and f states of O; 1.50 au for the s, p, d, and f states of Si; and 0.65 au for the s, p, d, and f states of H. The basis sets were single-ζ for the 3s semicore and 3p states of Ca and double-ζ plus a single shell of polarization functions for the Ca 4p as well as valence states of all the other atoms. The cutoff radii of the basis functions were determined using an energy shift[18] of 0.02 Ry. Partial core corrections[24] were used for Si to improve the transferability of the pseudopotential. The Brillouin zone was sampled using Monkhorst−Pack grids with reciprocal spacing of 0.8 $Å^{-1}$ or denser.[25]

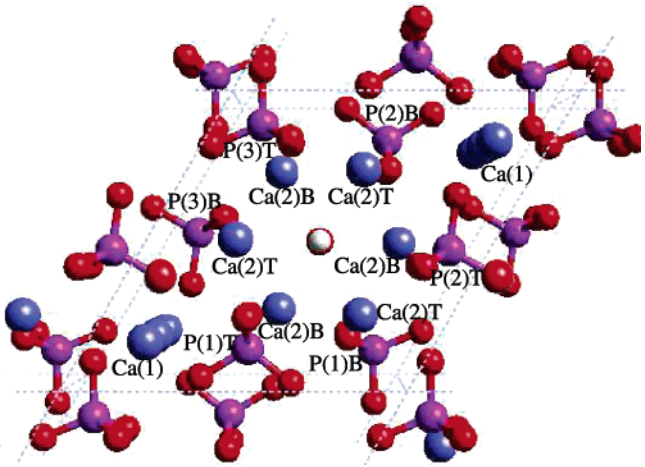

Figure 1. Structure of HA along the *c* axis. The color codes are P, purple; Ca, blue; O, red; and H, white. The positions of phosphorus marked with a T (top layer) are those closer to the remaining OH group when P is replace by Si, while those P positions marked with a B (bottom layer) are closer to the OH vacancy. The Ca(1) and Ca(2) denote column and triangle Ca atoms, respectively.

B. Structures and Techniques for Energy Comparisons. A unit cell of HA containing two formula units is illustrated in Figure 1. The schematized phosphate groups and the hydroxyls are labeled to identify the Si for P substitution sites and the OH vacancy which provides charge compensation in one of the systems studied. The structure is hexagonal with space group $P6_3/m$ and experimental lattice parameters $a = b = 9.4225$ Å and $c = 6.8850$ Å.[26] The OH are aligned and form a column along the *c* axis. There are two sorts of Ca. The Ca(1)'s form columns also along the *c* axis. The remaining six Ca(2)'s and the six PO_4 groups per cell lie in two layers parallel to the $a-b$ plane which are labeled T (top) and B (bottom) and form equilateral triangles about the OH column. During geometry optimizations, no symmetry constraints were imposed on the systems, and the $P6_3/m$ symmetry was often broken as a result of substitution-induced distortions. As noted earlier, monoclinic HA phases with doubled *b* lattice parameter have been observed, and the interactions between Si impurities and neighboring subcells may have interesting consequences on the defect formation energies and hexagonal−monoclinic phase stability. However, computational costs placed these effects beyond the scope of our work. We focused on local interactions between Si impurities, host lattice, and compensating defects, which can be treated reasonably well in a single-cell model, while multiple unit cell constructions were used only when it was critical for modeling dilute conditions and defect disorder, as explained below.

We consider first the substitution of Si for P with charge compensation by an excess hydrogen. A superlattice geometry is used in the calculations, in which the atoms of interest are located in one cell which is repeated to form a periodic superlattice. If a single hexagonal unit cell of HA containing two formula units is used as the superlattice cell, a single substitution of one Si per HA unit cell leads to quite a high Si concentration: 2.8 wt %. The H can be bound to different O atoms; three different H positions (1), (2), and (3) were investigated. The relaxed arrangements for these

(16) Hohenberg, P.; Kohn, W. *Phys. Rev. B* **1964**, *136*, 864.
(17) Kohn, W.; Sham, L. *Phys. Rev. A* **1965**, *140*, 1133.
(18) Soler, J. M.; Artacho, E.; Gale, J. D.; García, A.; Junquera, J.; Ordejón, P.; Sánchez Portal, D. *J. Phys.: Condens. Matter* **2002**, *14*, 2745−2779.
(19) Bazaraa, M. S.; Sherali, H. D.; Shetty, C. M. *Nonlinear programming: theory and algorithms*; John Wiley & Sons: New York, 1993.
(20) Perdew, J. P.; Burke, K.; Ernzerhof, M. *Phys. Rev. Lett.* **1996**, *77*, 3865.
(21) Troullier, N.; Martins, J. L. *Phys. Rev. B* **1991**, *43*, 1993.
(22) Yin, X.; Stott, M. J.; Rubio, A. *Phys. Rev. B* **2003**, *68*, 205205-13.
(23) Calderín, L.; Stott, M. J.; Rubio, A. *Phys. Rev. B* **2003**, *67*, 134106.
(24) Louie, S. G.; Froyen, S.; Cohen, M. L. *Phys. Rev. B* **1982**, *26*, 1738.
(25) Monkhorst, H. J.; Pack, J. D. *Phys. Rev. B* **1974**, *13*, 5188.
(26) *Standard Reference Materials Program*; National Institute of Standards and Technology: Gaithersburg, MD, 2003. Standard Reference Material 2910;

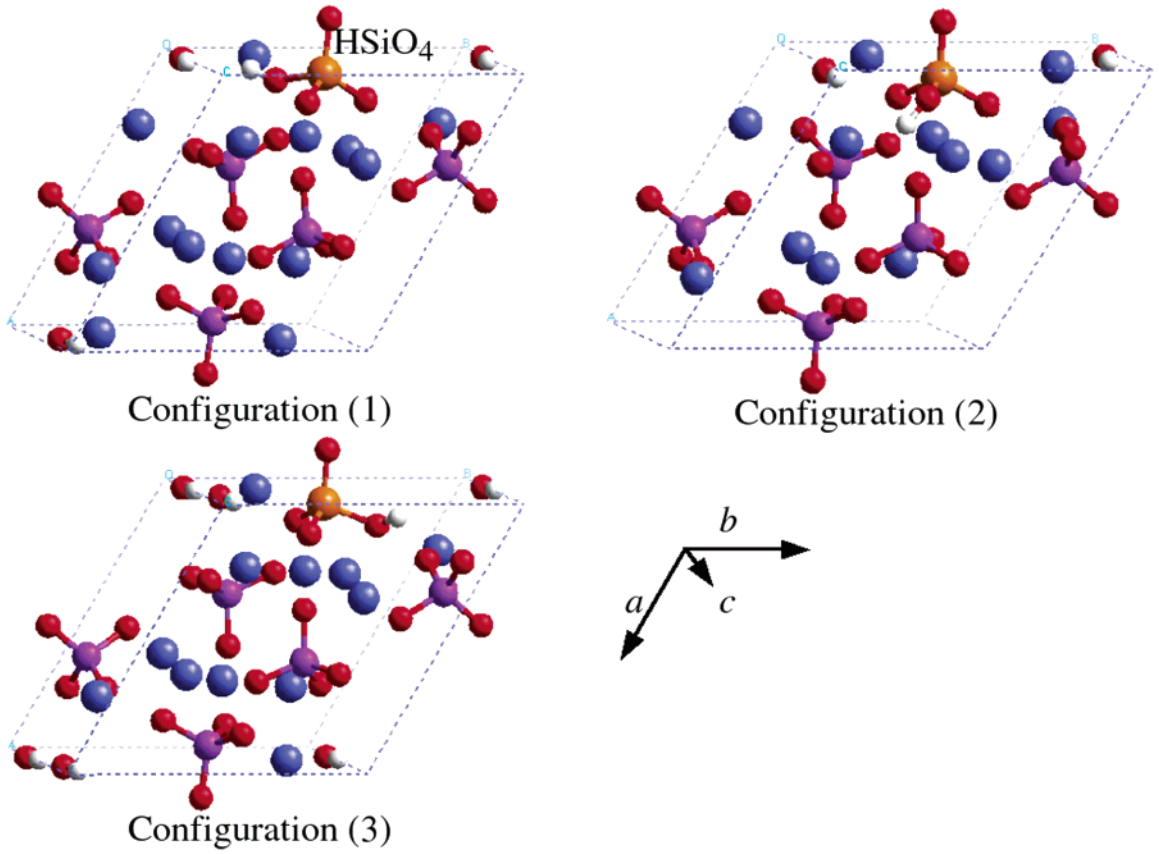

Figure 2. Relaxed $HSiO_4$-compensated structures. The orange sphere denotes the Si atom.

cases are illustrated in Figure 2. Furthermore, the $HSiO_4$ ion can occupy different symmetry equivalent sites, and substituting on one of these breaks the symmetry of the crystal because of the periodicity of the superlattice so that the *a* and *b* lattice parameters will become unequal. In the real crystal the hexagonal symmetry is restored by having a disordered arrangement of impurities. This can be simulated in the calculations by having a supercell consisting of several HA hexagonal unit cells and a disordered arrangement of impurities throughout the supercell cell, but at the cost of a more demanding calculation. In this study the effect of disorder was treated using a stack of three HA unit cells in the *c* direction, with a single $HSiO_4$ of configuration (1) in each cell. The disordered arrangement of impurities was modeled by placing the impurities in a spiraling arrangement along the channel, so that the HA unit cells were rotated by $\pm 120°$ with respect to their neighbors. Although this is of course an ordered structure it has the merit of preserving the hexagonal lattice of HA with equivalent *a* and *b* lattice parameters. Also, for completeness, an arrangement of the configuration (1) $HSiO_4$−HA where one of the channel OH ions was flipped was examined as this could lead to some bonding between the compensating H and the O of a channel OH. A double-cell arrangement of the configuration (1) $HSiO_4$ was studied to simulate more dilute conditions.

The second possibility considered here is a compensation of two SiO_4 impurities by an oxygen vacancy, V_O. In this case, the two SiO_4 groups and the vacancy can interact to form a Si_2O_7 complex. This complex was investigated in the study of Si-doped α-tricalcium phosphate where it was found to be bound.[15] Again, there are a number of distinguishable arrangements of the Si_2O_7 complex in a HA unit cell. A set of these was studied using a single cell host crystal. Because this system has twice the Si concentration as the other structures considered, a double cell calculation of the most stable configuration was performed in addition. The energetics of the $2SiO_4 + V_O$ substitution mechanism can be compared with that of the $HSiO_4$ case by noting that these two defects can transform to one another in a simple reaction involving water,

$$2SiO_4 + V_O + H_2O \leftrightarrow 2HSiO_4 \quad (1)$$

Another possibility that was considered in the earlier ab initio study of Si-doped α-tricalcium phosphate[15] was charge compensation of two SiO_4 groups by an excess Ca, the three forming a compact charge neutral defect. This possibility was not considered in the present study because in contrast to α-TCP there is no convenient vacant site in HA that can accommodate the addition of Ca, and the alternative interstitial Ca would heavily strain the lattice. Furthermore, the proportions of Ca, P, and Si in the Si−HA materials that have been reported[11−14] were carefully controlled, whereas there is uncertainty in the O and H content.

A third possible charge neutral substitution mechanism is SiO_4 substitution at the PO_4 site and the formation of an OH vacancy. With a particular one of the two OH's removed from the hexagonal unit cell of HA there are six possibilities for the substitution of a P by a Si, but these fall into two groups of three that are related by symmetry. One group has the SiO_4 in the same plane as the OH vacancy, and these three arrangements are identical through the symmetry [configurations P(1)B, P(2)B, and P(3)B]; the other group has the SiO_4 in the plane of the remaining OH [configurations P(1)T, P(2)T, and P(3)T]. As a check on the results of the simulations, all six arrangements were treated. This was done by removing the hydroxyl labeled B in Figure 1 and substituting a Si for the P in one of the six PO_4 groups. Full relaxation for each of these cases was performed. As in the case of the excess hydrogen charge compensation described above each of these systems breaks the hexagonal symmetry of the superlattice, and an additional simulation was performed with a supercell consisting of three HA unit cells stacked along the *c* axis with a spiraling arrangement of the defects of configuration (4) along the channel. Again, the $SiO_4 + V_{OH}$

defect can transform into the $2SiO_4 + V_O$ defect described above by another simple reaction involving water,

$$2SiO_4 + 2V_{OH} + H_2O \leftrightarrow 2SiO_4 + V_O \quad (2)$$

A final possibility considered here for charge compensation is the formation of a HPO_4 ion to accompany a substituted SiO_4 ion. This was investigated using a HPO_4 ion in a double unit cell. Such a pair of defects has the same stoichiometry as the $HSiO_4 + PO_4$, and, therefore, the total energies can be compared directly.

In addition to different Si−HA structures, pure HA, an isolated H_2O molecule in a $15 \times 15 \times 15$ Å^3 periodic box, and the ice I_c structure[27,28] made up of eight H_2O molecules with polarization in [001] direction were relaxed as reference systems required for the energy comparisons below.

The three charge compensation mechanisms SiO_4+V_{OH}, $2SiO_4 + V_O$, and $HSiO_4$ form a sequence

$$2SiO_4 + 2V_{OH} \xrightarrow{H_2O} 2SiO_4 + V_O \xrightarrow{H_2O} 2HSiO_4$$

where in each step the hydration proceeds by one H_2O unit. In a sequence such as this the defect formation energies can be compared by treating the chemical potential of water $\mu(H_2O)$ as a variable. The defect formation energies, F, can be defined in terms of chemical potentials μ and supercell energies E as

$$F(HSiO_4) = E(HSiO_4) - E(HA) + \mu(Si) - \mu(P) + \mu(H)$$

$$F(2SiO_4 + V_O) = E(2SiO_4 + V_O) - E(HA) + 2\mu(Si) - 2\mu(P) - \mu(O)$$

$$F(SiO_4 + V_{OH}) = E(SiO_4 + V_{OH}) - E(HA) + \mu(Si) - \mu(P) - \mu(O) - \mu(H) \quad (3)$$

The absolute values of formation energies are difficult to calculate because they depend on the full set of atomic chemical potentials. But, in energy comparisons most of these cancel out so that after regrouping the terms only $\mu(H_2O)$ is left undetermined, and formation energy differences relative to SiO_4−HA [$\Delta F(X) = F(X) - F(HSiO_4)$] can be written as

$$\Delta F(2SiO_4 + V_O) = E(2SiO_4 + V_O) + E(HA) - 2E(HSiO_4) - \mu(H_2O)$$

$$\Delta 2F(SiO_4 + V_{OH}) = 2E(SiO_4 + V_{OH}) - 2E(HSiO_4) - 2\mu(H_2O) \quad (4)$$

Thus, by plotting the formation energies as functions of $\mu(H_2O)$ and following the lowest energy envelope, we can determine which is the most stable defect at a given $\mu(H_2O)$. Furthermore, if the formation energy for a given defect is always above the envelope, then such a defect is not energetically stable.

III. Results

The results of the calculations are presented beginning with a comparison of the formation energies for the various charge compensation mechanisms. This is facilitated by using the observation, described in the previous section, that the three charge compensation mechanisms form a hydration sequence, where each step proceeds by the addition of one H_2O unit. This section continues with descriptions of the atomic arrangements and the various factors that determine relative energies of the different configurations. The results follow for the effects of Si doping on the lattice parameters and distortion indices for which experimental results are available.

Table 1. Supercell Energies for Configurations of Single Cell Substitutions, Pristine Bulk HA, H_2O Molecule and Ice[a]

	energy (eV)	difference (eV/Si)
$HSiO_4$−HA(1)	−23 504.10	+0.01
$HSiO_4$−HA(1), OH flipped	−23 504.02	+0.08
$HSiO_4$−HA(2)	−23 503.90	+0.20
$HSiO_4$−HA(3)	−23 504.10	0
$HSiO_4$−HA(1), double	−47 096.75	+0.10
HPO_4−HA, double	−47 095.52	+1.34
$HSiO_4$−HA(1), triple	−70 511.51	+0.27
$2SiO_4 + V_O$	−22 946.49	0
$2SiO_4 + V_O$, double	−46 538.94	+0.31
$SiO_4 + V_{OH}$(4)	−23 035.44	0
$SiO_4 + V_{OH}$(6)	−23 035.09	+0.34
$SiO_4 + V_{OH}$(4), triple	−69 105.22	+0.36
bulk HA	−23 592.75	

	energy (eV)	difference (eV/H_2O)
H_2O	−466.22	+1.49
ice	−3741.73	0

[a] The most stable Si−HA structures are in bold.

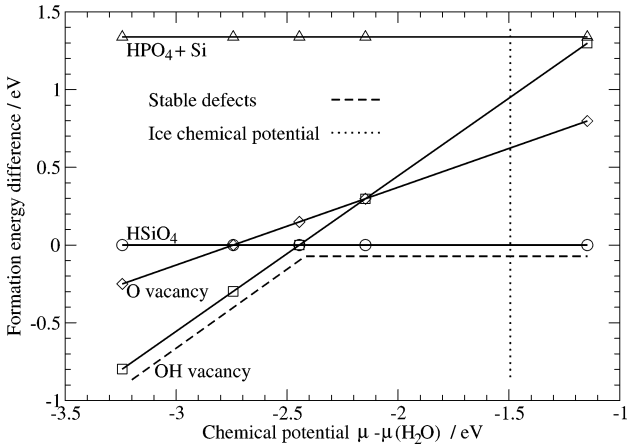

Figure 3. Formation energy differences of defects as a function of H_2O chemical potential $\mu(H_2O)$. The *y* axis has been scaled so that the formation energy of the $HSiO_4$-compensated defect is always zero. The *x* axis has been scaled so that the chemical potential of an isolated relaxed H_2O molecule is zero. The vertical dotted line marks the ice chemical potential giving a characteristic low value of $\mu(H_2O)$. The dashed line indicates the envelope that gives the most stable defect complex at a given chemical potential.

A. Energy Comparison. The supercell energies of the most stable defect configurations, as well as bulk HA, the free H_2O molecule, and ice, are presented in Table 1. Taking the lowest energies of these for each charge compensation mechanism and using eq 4, a formation energy difference plot has been produced and is shown in Figure 3. In the graph the values are normalized so that $F(HSiO_4) = 0$ and $\mu(H_2O) = 0$ for an isolated H_2O molecule, and the slopes are scaled so that the formation energies are per Si impurity per unit cell. The zero of the *x* axis reflects a high value of chemical potential at $T = 0$ K and $P = 0$ Pa, because no hydrogen bonding networks which would lower the energy can form for isolated H_2O. To estimate a characteristic low value of the water chemical potential for a fully hydrogen-bonded H_2O system, the calculated energy per molecule for the ice

(27) Lonsdale, K. *Proc. R. Soc. London, Ser. A* **1958**, *247*, 424.
(28) Lee, C.; Vanderbilt, D.; Laasonen, K.; Car, R.; Parrinello, M. *Phys. Rev. B* **1993**, *47*, 4863.

I_c structure was used. Note that upon relaxation the initially cubic cell shape of ice I_c distorted slightly.

When the energies for the three charge compensation mechanisms (V_{OH}, V_O, $HSiO_4$) are compared, we find that at low values of water chemical potential the V_{OH} compensation mechanism is energetically favored and at higher values the compensation by interstitial H leading to the formation of a $HSiO_4$ complex is favored. The formation energy differences relative to the $HSiO_4$ complex are plotted in Figure 3. The relative formation energy of the V_O-compensated defect is always slightly above the envelope, and it is, therefore, energetically unstable. But, a lowering of the energy of this system by as little as 0.2 eV per Si impurity would make the V_O mechanism stable over a narrow intermediate range of $\mu(H_2O)$. Because the $HSiO_4$- and HPO_4-compensated Si substitution have the same stoichiometry, their energies can be compared directly and the formation energy lines will be parallel. The energy of the HPO_4 + Si was found to be above that of $HSiO_4$, so the line representing the HPO_4 mechanism lies above that for $HSiO_4$ and also always lies above the envelope. The following discussion of the energies, atomic arrangements, and lattice parameters focuses particularly on those involving the $HSiO_4$ and the V_{OH} charge compensation mechanisms which give the stable envelope in Figure 3.

B. Stability and Atomic Structures. With $HSiO_4$, the two most stable configurations were (1) and (3). Configuration (3) was found by placing the H ion close to a PO_4 to form a HPO_4 ion; however, upon relaxation the H transferred from PO_4 to SiO_4 to form a $HSiO_4$. This transfer demonstrates the stronger affinity for H of the SiO_4 than the PO_4.

The three relaxed structures are presented in Figure 2. In configurations (1) and (3) the H was bound to O ions that flank the OH channel. In (1) the O had a weak bond to channel OH while in (3) the weak bond was to the neighboring PO_4 group in a layer above. The (3) configuration was nominally more stable, but the energy difference was so small that they can be considered equal. The (2) configuration, in which the H was bound to an O ion away from the channel, was less stable by 0.2 eV. Again, a weak bond formed between H and a PO_4 group in the layer above.

For structure (1), the inversion of the second OH group in the cell was found to increase the total energy slightly, by 0.1 eV. This small increase may stem from the competition between increased electrostatic repulsion and attraction between the extra H and the OH. Putting $HSiO_4$ groups in a spiral arrangement in the triple unit cell increases the energy by 0.3 eV per $HSiO_4$ but preserves the hexagonal unit cell shape with $a = b$, which was its intent. More dilute conditions were studied using a single configuration (1) $HSiO_4$ in a cell doubled in the c direction. Comparing the energies of the single cell plus a pure HA cell to double cell substitution (Table 1), it is found that the single cell complex has a lower energy by 0.1 eV per Si.

For structure (1), the bond length between the Si and the O in the OH group is 1.76 Å in a single cell, OH flipped single cell and double cell cases, and 1.77 Å for the triple cell. These are longer than we computed for an isolated $HSiO_4$ cluster (1.65 Å) and also longer than those typically found in bulk silica phases (1.6 Å).[29−31] The O−H bond length is slightly increased because of the attraction of the H toward the O atom belonging to the channel OH group, with bond lengths of 1.01−1.02 Å versus 0.96 Å in a calculated free $Si(OH)_4$ cluster. The H−OH distance between the impurity H and the channel O is relatively short: 1.59 Å for the single cell, 1.57 Å for the OH flipped single cell, 1.63 Å for the double cell, and 1.69−1.72 Å for the triple cell, suggesting at least a strong hydrogen bond. Also, the $HSiO_4$ could easily deprotonate so that a H_2O forms. We tested the possibility of a stable H_2O and a deprotonated SiO_4 ion; however, such a complex relaxes back to $HSiO_4$ and OH without a reaction barrier. For structure (2), the Si−(OH) distance is 1.77 Å and the (SiO)−H distance 0.99 Å. The (PO)−H distance to the neighboring PO_4 group is 1.82 Å, indicating a weaker bond than in structure (1). A similar bonding pattern is found for structure (3); the Si−(OH) distance is 1.75 Å, and the (SiO)−H distance is 1.00 Å. However, the (PO)−H distance to the neighboring PO_4 group is 1.69 Å, suggesting strong hydrogen bonding as was the case in structure (1).

Charge compensation by the hydrogen being associated with a PO_4 ion was also considered. In the single-cell case the H was transferred to SiO_4 as described above, but in a double cell, in which the HPO_4 was placed in one half of the double cell and the SiO_4 was placed in the other half, the HPO_4 was metastable. Upon relaxing this system the H stayed close to the PO_4, but the final energy was 1.2 eV higher than for a $HSiO_4$ complex in a double cell. The O−H bond length in the HPO_4 complex is 1.09 Å, and the H−OH bond length between the complex and the channel OH is 1.40 Å; the interstitial H is closer to the OH group than in the case of the $HSiO_4$ complex. This result further indicates that the PO_4 group has a weaker affinity for H than the SiO_4. The P−O bond length increases to 1.67 Å from about 1.6 Å in pristine HA.

For V_{OH} charge compensation, the final energies per cell are given in Table 1. Two groups were evident. Given the position of the OH vacancy, substitutions 3, 4, and 5 are equivalent in a hexagonal superlattice, as are 1, 2, and 6. Within the 3, 4, and 5 group, the total energies are identical to better than 0.01 eV per cell, which provides a check on the numerical procedures and the relaxations. The energy for the 3, 4, and 5 group of SiO_4 impurities is lower by 0.4 eV per cell than that for the other group. These favored anion positions in the HA structure lie in a layer normal to the c axis, and each of these is about 1.5 Å closer to the OH that was removed than to the remaining hydroxyl. The SiO_4 in each of these positions is much closer to the charge compensating OH vacancy than a SiO_4 in the other group, which accounts for the lower energy for the 3, 4, and 5 group. The most stable structure, structure (4), is presented in Figure 4. The energy of the spiral arrangement of SiO_4 in a triple unit cell is 0.4 eV per Si higher than for the most stable single-cell substitution [structure (4)], but the hexagonal unit cell shape of the HA is recovered to high precision.

In the V_O-compensated system there is a possibility that a Si_2O_7 complex is formed, lowering the energy. This is the complex found in earlier ab initio studies of Si-doped

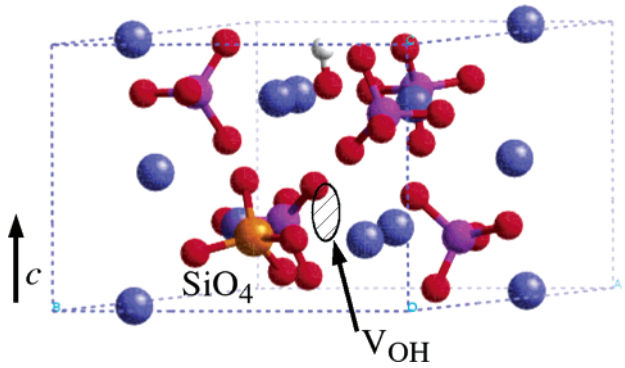

Figure 4. Side view of V_{OH}-compensated structure (4). The position of the vacant OH site is shown.

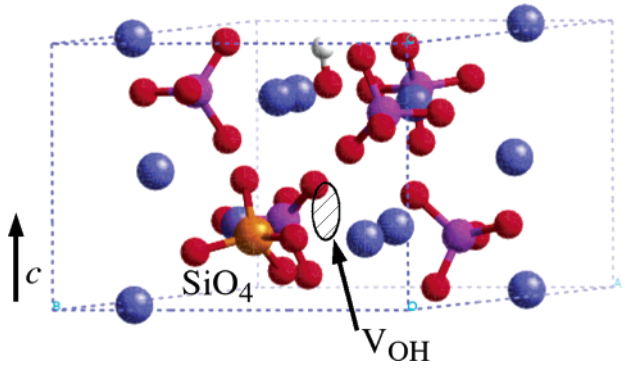

Figure 5. Side view of the most stable V_O-compensated structure: 2−5 configuration. The Si_2O_7 group has been highlighted.

α-tricalcium phosphate. There are several distinct initial arrangements of a SiO_3 and a SiO_4 in a HA unit cell, but relaxation gave a Si_2O_7 complex only in one case when phosphate groups 2 and 5 were substituted, and this gave the lowest energy configuration for the V_O charge compensation mechanism. This structure is presented in Figure 5. The Si_2O_7 complex that was formed for this 2−5 configuration has the Si atoms in a Q^1 configuration, with the Si−O interatomic distances for the bridging O at 1.77 and 1.75 Å being substantially larger than typical Si−O distances in bulk silica, and may indicate that the system is under local strain.[29−31] The Si−O bond lengths for nonbridging oxygens are 1.63−1.66 Å. The Si−O−Si bond angle is 119° which is much smaller than typical bond angles in bulk silica phases (>140°)[32] and those found for the Si_2O_7 complex in mineral rankinite, $Ca_3Si_2O_7$ (136.2°),[33] which further indicates that the system in Si−HA is locally strained. This charge compensation mechanism by an oxygen vacancy allowing the formation of a bound Si_2O_7 complex was found to be less favored energetically in Si-doped α-tricalcium phosphate than the other one considered involving excess Ca. There is the same finding here for Si-doped HA, but now the comparison is to different degrees of dehydration. For a wide range of reasonable values for the chemical potential of H_2O, charge compensation of substituted Si by an oxygen vacancy is energetically unstable. The lowest energy 2−5 configuration has the two Si's substituted in different phosphate layers, with the Si_2O_7 roughly aligned with the *c* axis. Another system with the two Si's in different phosphate layers has an energy 0.08 eV higher, but in this case the SiO_3 bonded to a neighboring PO_4 to form an $O_3Si-O-PO_3$ complex with the SiO_4 close by to provide charge compensation. Two other systems with the Si's substituted in the same HA phosphate layer were at still higher energies 0.13 eV above the lowest energy configuration. In one of these an $O_3Si-O-PO_3$ complex formed.

Table 2. Calculated Unit Cell Parameters of HA and Si-Doped HA

system	Si wt %	*a* (Å)	*b* (Å)	*c* (Å)	α (deg)	β (deg)	γ (deg)	Δ*V*/*V* (%)
HPO_4 (d)	1.4	9.412	9.424	13.965	90.3	88.8	119.6	0.52
Si_2O_7	5.7	9.357	9.425	6.950	91.7	89.9	119.8	0.38
Si_2O_7 (d)	2.8	9.353	9.425	13.934	91.5	89.9	119.8	0.27
SiO_4H (1)	2.8	9.427	9.272	6.980	90.8	88.6	119.0	0.72
$HSiO_4$ (3)	2.8	9.407	9.346	7.004	89.1	92.0	120.0	0.70
$HSiO_4$ (d)	1.4	9.390	9.316	13.957	90.7	88.9	119.6	0.28
$HSiO_4$ (t)	2.8	9.389	9.386	21.043	90.1	89.8	120.0	1.14
$SiO_4 + V_{OH}$	2.8	9.339	9.435	6.951	91.1	90.0	120.3	−0.16
$SiO_4 + V_{OH}$ (t)	2.8	9.363	9.363	20.952	90.0	90.0	120.0	0.17
pure HA	0	9.351	9.352	6.989	90.0	90.0	120.0	

Table 3. Lattice Distortions with Respect to HA Normalized to a Si wt % Content of 2.8

system	Δa (Å)	Δb (Å)	Δc (Å)	Δ*V*/*V* (%)
		theory		
HPO_4 (d)	0.122	0.144	−0.060	1.05
Si_2O_7	0.002	0.029	−0.016	0.18
Si_2O_7 (d)	0.002	0.040	−0.044	0.27
$HSiO_4$ (1)	0.076	−0.080	−0.009	0.72
$HSiO_4$ (3)	0.056	−0.006	0.015	0.70
$HSiO_4$ (d)	0.078	−0.072	−0.042	0.57
$HSiO_4$ (t)	0.038	0.034	0.025	1.14
$SiO_4 + V_{OH}$	−0.012	0.083	−0.038	0.15
$SiO_4 + V_{OH}$(t)	0.012	0.012	−0.005	0.17
		experiment		
Gibson et al.[11]	−0.021		0.385	−0.21
Ruys[10]	0.030		0.030	8.9
Kim et al.[12]	0.004		0.038	3.4
Leventouri et al.[13]	−0.0035		0.0469	3.29
Arcos et al.[14]	−0.0009		−0.0006	−0.149

C. Lattice Parameters. The relaxation of the atom positions and the supercell parameters gives values for the lattice parameters of the Si-doped HA. The calculated lattice parameters and the fractional change in volume for the most energetically favorable arrangements for the different charge compensation mechanisms studied are listed in Table 2, along with the calculated parameters for pure HA. The level of Si doping for the different systems is also listed (Table 3); 2.8 wt % of Si corresponds to one Si per HA unit cell, but some of the systems have smaller or greater concentrations. Measured lattice parameters reported by different groups for HA and single phase, hexagonal Si-doped HA and for HA Standard Reference Material[26] are given in Figure 6.

The calculated Si−O bond length is slightly larger than the P−O length resulting in a SiO_4 with about 15% larger volume than the PO_4 it substitutes for. This tends to increase the volume of the doped HA, but the charge compensating defect also affects the volume. The overall effect is a small volume increase in all cases except for the $SiO_4 + V_{OH}$ case for which there is a small decrease. The largest increases are for the case with charge compensation provided by an

(29) Levien, L.; Prewitt, C. T.; Weidner, D. J. *Am. Mineral.* **1980**, *65*, 920.
(30) Downs, R. T.; Palmer, D. C. *Am. Mineral.* **1994**, *79*, 9.
(31) Richardson, J. W.; Pluth, J. J.; Smith, J. V.; Dytrych, W. J.; Bibby, D. M. *J. Phys. Chem.* **1988**, *92*, 243.
(32) Astala, R.; Auerbach, S. M.; Monson, P. A. *J. Phys. Chem. B* **2004**, *108*, 9208.
(33) Saburi, S.; Kusachi, I.; Henmi, C.; Kawahara, A.; Henmi, K.; Kawada, I. *Mineral. J.* **1976**, *8*, 240.

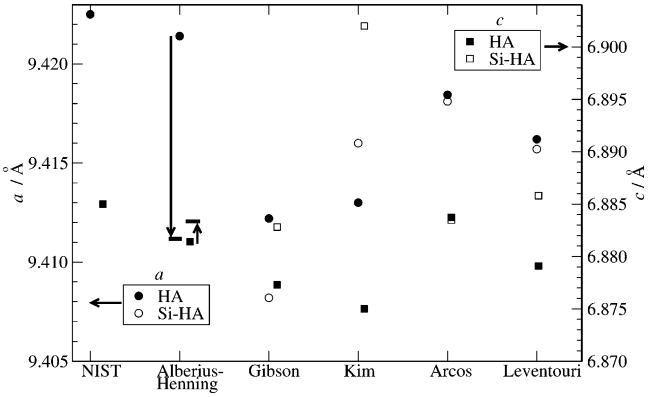

Figure 6. Graphical survey of the measured *a* and *c* lattice parameter results reported by various experimental groups for HA and Si-doped HA. Results are presented from Gibson et al.,[11] Kim et al.,[12] Leventouri et al.,[13] and Arcos et al.[14] Also illustrated are the ranges of results for *a* and *c* for HA and 39% dehydrated HA of Alberius-Henning et al.[34] Values of lattice parameters of NIST HA reference material 2910 are also indicated.[26]

additional H, the other cases involve either an O or an OH vacancy which compensates somewhat for the larger SiO_4.

Generally, *c* contracts upon doping with two exceptions that involve additional H, and there is no simple pattern for the changes in *a* and *b* although in all cases except one there is an overall increase in the area of the basal plane, leading to volume increase. There are simple rationales for the changes in some cases. The lowest energy arrangement for the $2SiO_4 + V_O$ mechanism has the two Si's in different PO_4 layers which are drawn together contracting the *c* axis as the Si_2O_7 complex is formed. For the lowest energy arrangement of the $SiO_4 + V_{OH}$ mechanism the Ca(2) triangle around the hydroxide vacancy is expanded as discussed by Alberius-Henning et al., leading to an expansion of the basal plane.[34] However, when comparing the magnitudes of the lattice parameter changes in Table 2 it must be recognized that the Si concentrations are not all the same and are very high in the cases involving Si_2O_7 in a single HA cell.

Measured lattice parameters for HA with zero Si concentration and for doped Si−HA, reported by various groups, are also given in the Table 2, and again there are different levels of Si doping. Suffice it to note for the moment that in all cases a hexagonal Bravais lattice is reported, whereas in almost all the simulations the unit cell is slightly distorted away from hexagonal with $a \neq b$ and small changes in the angles α, β, and γ from 90 and 120°. This distortion is a result of the superlattice geometry of the theoretical structures. When a particular charge compensation mechanism is to be studied and the corresponding arrangement of atoms is prepared in the supercell, this cell is repeated so that it is an ordered lattice that is simulated. In contrast, the real material will be disordered having a random arrangement of symmetry equivalent sites for the Si substitution and associated defects that will preserve the hexagonal symmetry on a macroscopic scale. Simulation of such a structure would require an inordinately large supercell. The systems labeled $HSiO_4$(t) and $SiO_4 + V_{OH}$(t) go some way toward simulating these structures by using three HA cells each containing one of the three symmetry equivalent atomic arrangements and stacking them along the *c* direction. The results for these systems show that this device has restored the hexagonal unit cell shape, close to $a = b$ and $\alpha = \beta = 90°$ and $\gamma = 120°$. We note that *c* increases in one case and is effectively unchanged in the other, bucking the general trend of decreasing *c* seen for the other systems.

(34) Alberius-Henning, P.; Adolfsson, E.; Grins, J.; Fitch, A. *J. Mater. Sci.* **2001**, *36*, 663.

Table 4. Average Distortion Indices for All the PO_4 and SiO_4 Together (XO_4 av) and for the SiO_4 Groups Alone (SiO_4 av)

	XO_4 av		SiO_4 av	
system	D_{RMS} (deg)	D_{ABS} (deg)	D_{RMS} (deg)	D_{ABS} (deg)
HPO_4 (d)	2.89	2.57	4.25	3.90
Si_2O_7	3.77	3.29	6.15	5.45
Si_2O_7 (d)	3.09	2.73	6.64	5.88
$HSiO_4$ (1)	3.27	2.92	6.61	5.55
$HSiO_4$ (3)	3.14	2.86	5.59	4.96
$HSiO_4$ (d)	2.76	2.46	6.35	5.35
$HSiO_4$ (t)	2.84	2.55	6.13	5.34
$SiO_4 + V_{OH}$	3.79	3.37	7.15	6.37
$SiO_4 + V_{OH}$(t)	3.46	3.06	6.64	5.88
pure HA	2.04	2.01		

The distortion index is a measure of the distortion of the XO_4 cations from regular tetrahedra. In terms of the actual O−X−O bond angles θ_i and a reference angle θ_0 the distortion index can be defined either as a root-mean-square difference

$$D_{RMS} = \sqrt{\frac{1}{6}\sum_{i=1}^{6}(\theta_i - \theta_0)^2} \quad (5)$$

or as an absolute value difference

$$D_{ABS} = \frac{1}{6}\sum_{i=1}^{6}|\theta_i - \theta_0| \quad (6)$$

In either case θ_0 may be taken to be the average over all O−X−O bond angles or over those for the particular tetrahedron or the Platonic tetrahedron value $\theta_0 = \cos^{-1}(-1/3)$, which we have used. The square of D_{RMS} above has also been used. Calculated distortion indices are given in Table 4 for the most energetically stable systems of the types studied. Values for both D_{RMS} and D_{ABS} are given, and although the former is consistently the larger the patterns are similar. Average values over all XO_4 tetrahedra, SiO_4 as well as PO_4, are listed, and these may be compared with the calculated values for pure HA. Doping is seen to increase the distortion index by a factor of 1.5−2 over that for HA, with the largest increases for the Si_2O_7 system in which there are two Si for P substitutions per HA cell, and the $SiO_4 + V_{OH}$ system. The distortion indices for the SiO_4 groups alone are also given, and evidently these contribute significantly to the XO_4 average values. The reductions in *D* for the Si_2O_7 and $HSiO_4$ systems, when they are placed in a double HA unit cell, and detailed analysis of the atomic coordinates show that the distortion of the PO_4 groups is greatest for those near the Si dopant and its accompanying charge compensating defects. Consequently, for weak doping the change of the distortion indices from the HA values on doping is likely to be proportional to the Si concentration.

IV. Discussion and Conclusions

The substitution of Si for P in HA produces a charge imbalance that can be rectified by the presence of a charge compensating defect. To be effective this defect must be closely associated with the Si dopant. Earlier calculations for carbonate HA suggest that the cost in energy of separating the compensating defect from an impurity could be over 5 eV.[35] However, there are many possible mechanisms for charge compensation; the most likely of these are the subject of this study. The simulations considered different mechanisms for charge compensation involving an OH vacancy and a HPO_4 group, also compensation for two substituted Si by an oxygen vacancy, and the possibility of $HSiO_4$ formation. An excess Ca could compensate for two Si; however, this does not seem to be a possibility in the materials of interest, and this system was not considered.

The observation that the mechanisms considered are linked one to the other by the addition of H_2O together with the calculated values for the total formation energies leads to the comparisons presented in Figure 3. The conclusion is that in equilibrium the formation of $HSiO_4$ is the stable mechanism for large values of the water chemical potential and for small values the OH vacancy mechanism is the stable one. Compensation by HPO_4 is excluded, and the total energy results also exclude the oxygen vacancy mechanism; however, a lowering of the formation energy of this system by as little as 0.2 eV due perhaps to an improvement in the basis set, the treatment of exchange and correlation, or inclusion of entropic effects would render the oxygen vacancy mechanism the most stable in a small intermediate range of water chemical potentials. Thus, our results support the experimental results of Arcos in the sense that additional H can bind to tetrahedral groups;[14] however, formation of $HSiO_4$ groups is energetically greatly favored over formation of HPO_4. It appears likely that the charge compensation mechanism for Si substituted for P depends on the availability of water during the manufacturing process, with different processes placing the material in different ranges of the water chemical potential and leading to different forms of Si−HA. But, it is unlikely that the manufacture of the material in a particular case, consisting of various stages, will lead to a single charge compensation mechanism.

The changes in lattice parameters on doping HA with Si is one possible area of comparison between theory and the experimental results. However, a direct comparison is hindered because the changes must depend on the level of doping which is not the same in different theoretical systems and the experimental materials. Furthermore, Si−HA is a polycrystalline material which further complicates comparisons between experimental and theoretical (single-crystal) results. The variation in doping level is remedied in an approximate way by invoking Vegard's law and linearly scaling all the theoretical and experimental results to a common doping level of 2.8 wt %, equivalent to one Si per HA unit cell. The results for the changes in *a*, *b*, and *c* and the percentage volume change are given in Table 3. There is some consistency in the theoretical results which show a small volume increase except in one case, *c* shrinking except for two cases, and the results for the two triple cell systems which have hexagonal cell shape with $a = b$ and which bear closest comparison with experiment, both showing volume increases but one contracting along *c* and the other expanding. But, there is no consistency in the experimental results. The normalized lattice parameter changes are positive in some cases and in others negative. Only Arcos et al. report a decrease in *c* which is generally the case for the theoretical results, but the changes in both *a* and *c* and in the volume are much smaller than for the other groups. From simple volume considerations it is expected that material compensated by additional H would have the largest volume expansion and V_{OH}-compensated material would have the smallest. This is because of the degree of dehydration; that is, the material compensated by additional H has the most dissociated water in the lattice, leading to volume expansion. Such a trend is indeed observable in Table 3.

The differences in observed lattice parameter changes may indicate differences in the types of Si−HA that have been prepared. However, there is considerable variation in the measured lattice parameters of the zero Si-doped materials, that is, for the HA prepared by the different groups. The HA-like material as well as the Si−HA may depend significantly on the method of preparation. These variations are illustrated graphically in Figure 6, which shows the measured *a* and *c* lattice parameters for the HA and the change upon Si doping for the different materials. Evidently there is as much variation in the HA lattice parameters as there is change upon doping with Si. Also shown in Figure 6 are the lattice parameters for the NIST HA reference material 2910, prepared by low-temperature precipitation. The measured *a* lattice parameters of all the examples of the HA-like material are significantly smaller than that for the standard material. Alberius-Henning et al. have carried out a systematic study of the structure of HA as it was dehydrated.[34] The values they report for HA before dehydration are shown in Figure 6 and are close to the values for the standard material. The lines directed from these values of *a* and *c* illustrate the changes in the *a* and *c* values upon dehydration and terminate at the measured values for the 39% dehydrated material. The *a* lattice parameter decreases substantially upon dehydration, while *c* increases a little. The range of values of *a* from zero to 39% dehydration measured by Alberius-Henning et al. covers all the values of the HA-like material reported in connection with Si−HA. The small change in *c* upon dehydration is consistent with the small scatter in *c* for the HA-like materials and the various forms of Si−HA.

The variation in the measured lattice parameters of the HA-like material and the reported changes, particularly in *a*, on dehydration suggest that the different methods of preparing HA and also probably Si−HA have resulted in different levels of hydration and possibly other defects in the materials. Indeed, Leventouri et al.[13] reported the OH occupancy of their HA-like material to be 0.30, much less than the expected value of 0.50. Without more information on the composition of the HA and Si−HA a detailed comparison of the changes in lattice parameters on Si doping

(35) Astala, R.; Stott, M. J. *Chem. Mater.* **2005**, *17*, 4125.

with the results of the simulation may not be possible. A more useful comparison of Si−HA with HA may be of the reported Si−HA with the NIST standard material or with the fully hydrated material of Alberius-Henning et al.[34] whose lattice parameters are very close to those of the standard material. This would eliminate the uncertainty arising from the differences in the HA-like materials. If this were a more appropriate comparison, then Figure 6 suggests that *a* decreases substantially on doping with Si, with little change in *c*. But, this does not support the results of the simulation. A more realistic interpretation is that the prepared Si−HA as well as the HA-like material is heavily defective. Our preliminary calculations for 50% dehydrated HA show that at $T = 0$ K, and low values of H_2O chemical potential, less than −4 eV on the scale of Figure 3, are required for phase stability. Thus, in conditions where dehydrated HA is present, V_{OH}-compensated Si−HA could form. However, dehydrated HA is likely to have complex properties that require further investigation.

Some experimental estimates of distortion indices obtained from analyses of X-ray or neutron scattering data have been reported, and these provide another possible point of contact between experiment and theory.[11,14,36] But, a direct comparison theory and experiment is again hindered by the different Si doping levels in the Si−HA and variations in the definition of the index.

To conclude, we have studied the defect chemistry of Si-doped HA using electronic structure total energy calculations. The focus was on resolving discrepancies concerning the behavior of lattice parameters and charge compensation mechanisms. Our results show two compensation mechanisms that are favorable, depending on the processing conditions. Under hydrating conditions formation of $HSiO_4$ groups is preferred, while in the dehydrating case, OH vacancies are preferred, showing that there is no unique composition of Si−HA and the experimental results will depend on conditions during sample preparation. It is of future interest how the properties of Si−HA are affected by different intrinsic defects and surface properties in crystallite samples.

Acknowledgment. This work was supported by the Natural Sciences and Engineering Council of Canada and Millenium Biologix Corp. Discussions with Dr. J. Reid are also acknowledged.

CM051989X

(36) Jha, L. J.; Best, S. M.; Knowles, J. C.; Rehman, I.; Santos, J. D.; Bonfield, W. *J. Mater. Sci.: Mater. Med.* **1997**, *8*, 185.